J|A|C|S
ARTICLES
Published on Web 05/26/2004

Partitioning of Dual-Lipidated Peptides into Membrane Microdomains: Lipid Sorting vs Peptide Aggregation

Sascha Janosch,[†] Chiara Nicolini,[†] Björn Ludolph,[‡] Carsten Peters,[‡] Martin Völkert,[‡] Theodore L. Hazlet,[§] Enrico Gratton,[§] Herbert Waldmann,[‡] and Roland Winter*,[†]

Contribution from the Department of Chemistry, Physical Chemistry I, University of Dortmund, Otto-Hahn-Strasse 6, D-44227 Dortmund, Germany, Max-Planck-Institute of Molecular Physiology, Otto-Hahn-Strasse 11, D-44227 Dortmund, and Laboratory for Fluorescence Dynamics, University of Illinois, Urbana, Illinois 61801

Received January 6, 2004; E-mail: roland winter@uni-dortmund.de

Abstract: The lateral membrane organization and phase behavior of the lipid mixture DMPC(di-C_{14})/DSPC-(di-C_{18})/cholesterol (0−33 mol %) with and without an incorporated fluorescence-labeled palmitoyl/farnesyl dual-lipidated peptide, BODIPY-Gly-Cys(Pal)-Met-Gly-Leu-Pro-Cys(Far)-OMe, which represents a membrane recognition model system for Ras proteins, was studied by two-photon excitation fluorescence microscopy. Measurements were performed on giant unilamellar vesicles (GUVs) over a large temperature range, ranging from 30 to 80 °C to cover different lipid phase states (all-gel, fluid/gel, liquid-ordered, all-fluid). At temperatures where the fluid−gel coexistence region of the pure binary phospholipid system occurs, large-scale concentration fluctuations appear. Incorporation of cholesterol levels up to 33 mol % leads to a significant increase of conformational order in the membrane system and a reduction of large domain structures. Adding the peptide leads to dramatic changes in the lateral organization of the membrane. With cholesterol present, a phase separation is induced by a lipid sorting mechanism owing to the high affinity of the lipidated peptide to a fluid, DMPC-rich environment. This phase separation leads to the formation of peptide-containing domains with high fluorescence intensity that become progressively smaller with decreasing temperature. As a result, the local concentration of the peptide increases steadily within the confines of the shrinking domains. At the lowest temperatures, where the acyl-chain order parameter of the membrane has already drastically increased and the membrane achieves a liquid-ordered character, an efficient lipid sorting mechanism is no longer supported and aggregation of the peptide into small clusters prevails. We can conclude that palmitoyl/farnesyl dual-lipidated peptides do not associate with liquid-ordered or gel-like domains in phase-separated bilayer membranes. In particular, the study shows the interesting ability of the peptide to induce formation of fluid microdomains at physiologically relevant cholesterol concentrations, and this effect very much depends on the concentration of fluid vs ordered lipid molecules.

Introduction

The structure and lateral organization of the lipid and protein constituents in biological membranes poses one of the major current problems in membrane biochemistry and biophysics. [1−15] Central questions in this area are related to the existence of lipid domains and the relationship between lipid-domain formation and the conformation and functional properties of membrane-associated proteins.[16−26] Formation of lipid domains is a mere

[†] University of Dortmund.
[‡] Max-Planck-Institute of Molecular Physiology.
[§] University of Illinois.

(1) Bagatolli, L. A.; Gratton, E *Biophys. J.* **2000**, *78*, 290−305.
(2) Bagatolli, L. A.; Gratton, E. *Biophys. J.* **2000**, *79*, 434−447.
(3) Bultmann, T.; Vaz, W. L. C.; Melo, E. C. C.; Sisk, R. B.; Thompson, T. E. *Biochemistry* **1991**, *30*, 5573−5579.
(4) Czeslik, C.; Erbes J.; Winter, R. *Europhys. Lett.* **1997**, *37*, 577−582.
(5) Jørgensen, K.; Mouritsen, O. G. *Biophys. J.* **1995**, *95*, 942−954.
(6) Jørgensen, K.; Klinger, A.; Biltonen, R. L. *J. Phys. Chem. B* **2000**, *104*, 11763−11773.
(7) Leidy, C.; Wolkers, W. F.; Jørgensen, K.; Mouritsen, O. G.; Crowe, J. H. *Biophys. J.* **2001**, *80*, 1819−1828.
(8) Nielsen, L. K.; Vishnyakov, A., Jørgensen, K.; Bjørnholm, T.; Mouritsen, O. G. *J. Phys.: Condens. Matter.* **2000**, *12*, A309−A314.
(9) Parasassi, T.; Gratton, E.; Yu W.; Wilson, P.; Levi, M. *Biophys. J.* **1997**, *72*, 2413−2429.
(10) Sugár, I. P.; Thompson, T. E.; Biltonen, R. L. *Biophys. J.* **1999**, *76*, 2099−2110.
(11) Winter, R.; Gabke, A.; Czeslik, C.; Pfeifer, P. *Phys. Rev. E.* **1999**, *60*, 7354−7359.
(12) Heerklotz, H.; Szadkowska, H.; Anderson, T.; Seelig, J. *Biophys. J.* **2003**, *329*, 793−799.
(13) Korlach, J.; Schwille, P.; Webb, W. W.; Feigensen, G. W. *Proc. Natl. Acad. Sci. U.S.A.* **1999**, *96*, 8461−8466.
(14) Simons, K.; Ikonen, E. *Nature* **1997**, *387*, 569−572.
(15) Edidin, M. *Annu. Rev. Biophys. Biomol. Struct.* **2003**, *32*, 257−283
(16) Cornelius, F. *Biochemistry* **2001**, *40*, 8842−8851.
(17) Curran, A. R.; Templer, R. H.; Booth, P. J. *Biochemistry* **1999**, *38*, 9328−9336.
(18) Davies, S. M. A.; Epand, R. M.; Kraayenhof, R.; Cornell, R. B. *Biochemistry* **2001**, *40*, 10522−10531.
(19) Dumas, F.; Sperotto, M. M.; Lebrun, M.-C.; Tocanne, J.-F.; Mouritsen, O. G. *Biophys. J.* **1997**, *73*, 1940−1953.
(20) Estrela-Lopis, I.; Brezesinski, G.; Möhwald, H. *Phys. Chem. Chem. Phys.* **2000**, *2*, 4600−4604.
(21) Hinderliter, A.; Almeida, P. F. F.; Creutz, C. E.; Biltonen, R. L. *Biochemistry* **2001**, *40*, 4181−4191.
(22) Sankaram, M. B.; Marsh, D.; Gierasch, L. M.; Thompson, T. E. *Biophys. J.* **1994**, *66*, 1959−1968.
(23) Schram, V.; Thompson, T. E. *Biophys. J.* **1997**, *72*, 2217−2225.
(24) Zein, M.; Winter, R. *Phys. Chem. Chem. Phys.* **2000**, *2*, 4545−4551.
(25) van der Goot, F. G.; Harder, T. *Semin. Immunol.* **2001**, *13*, 89−97.
(26) Wang, T.-Y.; Leventis, R.; Silvius, J. *Biophys. J.* **2002**, *79*, 919−933.

10.1021/ja049922i CCC: $27.50

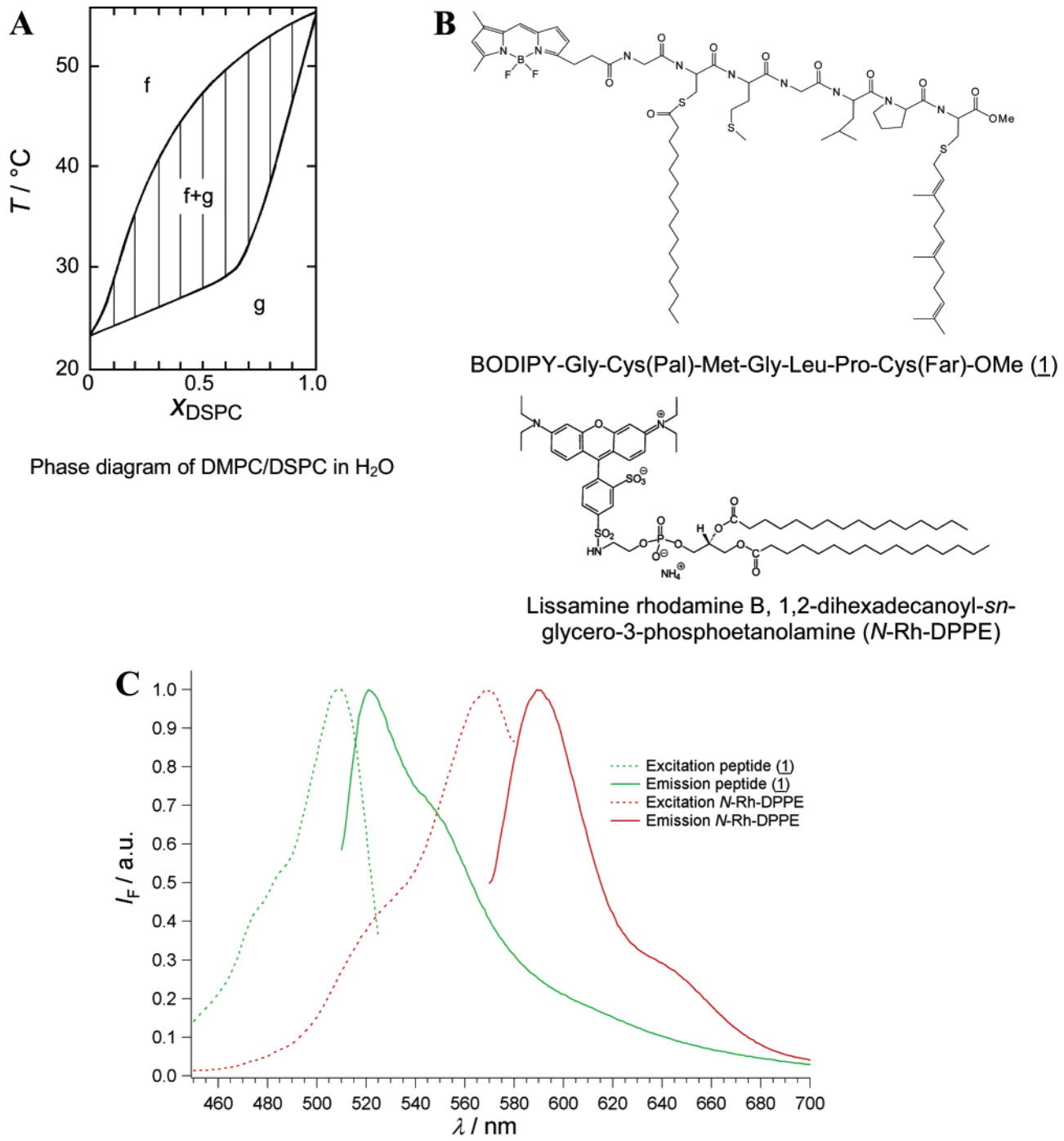

Figure 1. (A) Phase diagram of DMPC/DSPC in H_2O (f, fluid phase; g, gel phase; f+g, gel−fluid two-phase coexistence region). (B) Chemical structures of the lipidated peptide (**1**) (labeled with the fluorophor BODIPY) and the lipid fluorophor *N*-Rh-DPPE. (C) Excitation and emission spectra of the peptide (**1**) and *N*-Rh-DPPE.

consequence of the many-particle nature of biological membranes. In the state of equilibrium, lipid phase separation leads to the formation of macroscopically large domains (phases), whereas out of equilibrium the phase separation process may produce small-scale domains and extended compositional fluctuations may be observed. Solid experimental and theoretical evidence is available now that supports the existence of this type of heterogeneity already in two-component lipid bilayer systems, such das DMPC/DSPC (Figure 1A).[1−11] In recent years, substantial evidence has accumulated that points to the presence of distinct lipid regions in cell membranes termed rafts, which are rich in sphingomyelin and cholesterol. They are thought to contain liquid-ordered domains and to be important for cellular functions such as signal transduction and the sorting and transport of lipids and proteins.[14,15,25,27] To understand better the role of lipid complexes/clusters in regulating membrane properties, ternary mixtures of cholesterol and two lipids are often used in model studies.

In the present paper we explore the effects of a fluorescent peptide containing a farnesyl (Far) and palmitoyl(Pal) anchor, BODIPY-Gly-Cys(Pal)-Met-Gly-Leu-pro-Cys(Far)-OMe (**1**) (Figure 1B) which represents a membrane recognition model system

(27) Munro, S. *Cell* **2003**, *115*, 377−388.

for Ras proteins, on model membranes consisting of binary and ternary lipid mixtures. Specifically, we examine the peptide influence on lipid lateral organization and concentration fluctuations, and the possibility of molecular sorting of lipids by the embedded peptide. The model system consists of the binary phospholipid mixture DMPC/DSPC (1:1 mol/mol) with acyl-chains di-C_{14} (DMPC, dimyristoyl-phosphatidylcholine) and di-C_{18} (DSPC, distearoyl-phosphatidylcholine) and varying levels of cholesterol ranging from 0 to 33 mol %. The two phospholipid species have different hydrophobic chain lengths and show substantial temperature-dependent changes within a bilayer structure. The gel-to-fluid phase transition of these phospholipids is accompanied by an average decrease of ca. 4 Å in lipid length due to the increase in the population of gauche conformers and kinks in the lipid acyl-chains. In the gel phase the hydrocarbon chains are in a straight, elongated conformation; in the fluid phase, they are conformationally disordered (chain melting transition). The large difference in hydrophobic length (4 CH_2 groups) between the two lipid species implies a strongly nonideal mixing behavior and, therefore, results in a broad two-phase coexistence region between the gel and all-fluid phase states.[11,28] The particular regions of interest in this study are the heterogeneous phase-separated regions. Measurements of fluorescence recovery after photobleaching have indicated the existence of highly heterogeneous gel and fluid domains in the coexistence region of DMPC/DSPC.[3] Monte Carlo computer simulations of phase diagrams have exhibited long-lived percolation-like gel and fluid domains with a network of interfacial regions that have properties different from those of coexisting bulk phases.[29,5] Recently, small-angle neutron diffraction (SANS) experiments with multilamellar vesicles have shown the presence of large-scale surface-fractal domains in the two-phase region.[4,11] The data provided the first direct evidence that phase separation in multilamellar membranes is dominated by long-lived nonequilibrium structures, that these ramified structures have distinct boundaries, and that their formation is governed by interlamellar interactions.

Ras proteins function as molecular binary switches in biological signal transduction processes.[30] The Ras signaling pathway is central to the regulation of cell growth and differentiation, and impaired Ras function can be one of the critical steps leading to cell transformation. The importance of the correct functioning of the Ras cascade is illustrated by the fact that a point mutation in the ras oncogenes, usually in N- or K-Ras, is found in approximately 30% of all human cancers. To perform their normal and oncogenic functions, Ras proteins must be membrane associated. Their membrane targeting and membrane binding is controlled by a post-translational covalent attachment of lipid groups to the Ras proteins. Lipidation is believed to play a role in regulatory functions, e.g., by mediating protein−protein and protein−lipid interactions. The association with different membrane microenvironments is believed to further regulate Ras signaling mechanisms. In this context, it has also become clear that the differential lateral segregation of Ras isoforms, namely N-, H-, and K-Ras, would offer a plausible mechanism for how these highly homogeneous proteins generate distinct signal outputs.[31] Specific lipid modifications of proteins are believed to be sufficient to sequester them in certain microdomains, such as lipid rafts and caveolae. It has been shown for *Aequorea* fluorescent proteins with different types of lipid anchors that the myristoyl and palmitoyl groups promote clustering in rafts whereas isoprenyl groups do not.[32] Additionally, not only the structure of lipid modifications but also the position of their attachment seems to influence the affinity for specific membrane domains, at least in small model peptides.[33] Therefore, the question arises how the lipidation pattern of palmitoylated and farnesylated Ras proteins affects their localization to membrane microdomains and of what kind these domains may be.

In this work we are focusing on the effect of incorporation of the fluorescent (BODIPY) labeled lipidated peptide (**1**) (Figure 1B), which represents the fully post-translational processed C-terminus of N-Ras and anchors the N-Ras protein to the membrane, on the phase behavior and lateral organization of DMPC/DSPC/cholesterol mixtures, which—depending on concentration and temperature—provide all-fluid, all-gel, fluid−gel, and liquid-ordered heterogeneous lateral lipid bilayer structures. Vice versa, the effect of the lipid phase state and lateral organization on the partitioning of the lipidated peptide is studied. To observe the heterogeneous membrane structure and lipid concentration fluctuations, two-photon excitation fluorescence microscopy techniques are used,[1,2] complemented by fluorescence spectroscopy data to determine the fluorescence properties of the BODIPY-labeled peptide.

Materials and Methods

Materials and Sample Preparation. A. Lipids. 1,2-Dimyristoyl-*sn*-glycero-3-phosphatidylcholine (DMPC) and 1,2-distearoyl-*sn*-glycero-3-phosphatidylcholine (DSPC) were purchased from Avanti Polar Lipids (Birmingham, AL) and cholesterol from Sigma-Aldrich (Deisenhofen). The chemicals were used without further purification.

B. Peptides. Synthesis of BODIPY-Gly-Cys(Pal)-Met-Gly-Leu-Pro-Cys(Far)-OMe (1). Peptide (**1**) was prepared by a combination of solid-phase and solution-phase synthesis. As previously reported, the farnesylated and palmitoylated peptide Trt-Gly-Cys(Pal)-Met-Gly-Leu-Pro-Cys(Far) was built up on solid support using the phenylhydrazide linker strategy.[34] After oxidative release from the resin, the crude peptide was purified with column chromatography. Subsequent treatment of the peptide with a mixture of acetic acid and trifluoroethanol in CH_2Cl_2 led to cleavage of the N-terminal trityl group. The solvent was removed under reduced pressure and the residue coevaporated with toluene and dried in vacuo. The liberated amino group was acetylated with a preactivated solution of BODIPY-OH^{FL} (1.5 equiv), *N*-(3-dimethylaminopropyl)-*N*′-ethylcarbodiimid-hydrochloride (EDC, 1.5 equiv), and 1-hydroxybenzotriazole (HOBt, 2 equiv) in CH_2Cl_2 and in the presence of triethylamine (1.7 equiv). After purification by means of column chromatography, the target peptide (**1**) was obtained in 31% overall yield. TLC = 0.21 (CH_2Cl_2/methanol 20:1); ^{1}H NMR (500 MHz, $CDCl_3$) δ = 7.03 (s, 1H, BODIPY), 6.80 (s, 1H, BODIPY), 6.20 (s, 1H, BODIPY), 6.03 (s, 1H, BODIPY), 5.03−5.10 (m, 1H, C═CH Far), 5.02−4.94 (m, 2H, C═CH Far), 4.64−3.90 (m, 9H, 5 × α-CH, 2 × α-CH_2 Gly, β-CH_{2a} Ser), 3.83−3.44 (m, 8H, β-CH_{2b} Ser, CH_2 Pro, OMe, CH_2 BODIPY), 3.22−2.78 (m, α-CH_2 Far, β-CH_2 Cys), 2.70−2.42 (m, 9H, CH_3, CH_2 BODIPY, α-CH_2 Pal, γ-CH_2 Met), 2.16 (m,

(28) Mabrey, S.; Sturtevant, J. M. *Proc. Natl. Acad. Sci U.S.A.* **1976**, *73*, 3862−3866.
(29) Jørgensen, K.; Sperotto, M. M.; Mouritsen, O. G.; Ipsen, J. H.; Zuckermann, M. J. *Biochim. Biophys. Acta* **1993**, *1152*, 135−145.
(30) Wittinghofer, A.; Waldmann, H. *Angew. Chem., Int. Ed.* **2000**, *39*, 4193−4214.
(31) Hancock, J. F. *Nature Rev. Mol. Cell Biol.* **2003**, *4*, 373−383.
(32) Zacharias, D. A.; Violin, J. D.; Newton, A. C.; Tsien, R. Y. *Science* **2002**, *296*, 913−916.
(33) Wang, T.-Y.; Leventis, R.; Silvius, J. R. *Biochemistry* **2001**, *40*, 13031−13040.
(34) Ludolph, B.; Waldmann, H. *Chem. Eur. J.* **2003**, *9*, 3683−3691.

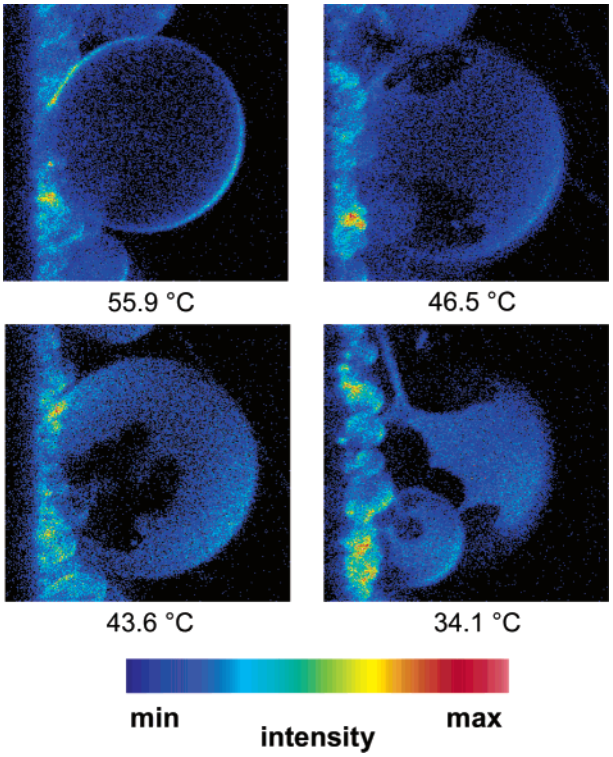

Figure 2. Two-photon excitation fluorescence intensity images (false color representation) of GUVs (size ~30 μm) formed of DMPC/DSPC (1:1) and labeled with *N*-Rh-DPPE. The images were taken at the top part of the GUVs at different temperatures. Below 49 °C, the gel−fluid two-phase region appears. The fluorescence label essentially partitions in the fluid phase only.

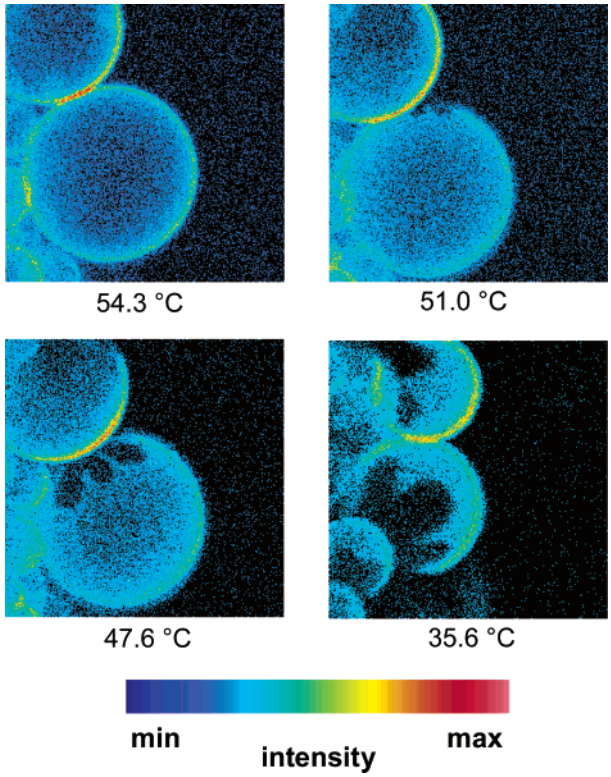

Figure 3. Two-photon excitation fluorescence intensity images (false color representation) of GUVs (size ~30 μm) formed of DMPC/DSPC (1:1) + 2 mol % of peptide (**1**). The images were taken at the top part of the GUVs at different temperatures. The BODIPY-labeled fluorescence peptide partitions essentially in fluidlike domains, only.

3H, CH_3 BODIPY), 2.04−1.82 (m, 17H, 4 × CH_2 Far, 2 × CH_2 Pro, β-CH_2 Met, SCH_3), 1.70−1.35 (m, 17H, γ-CH Leu, β-CH_2 Leu, 4 × CH_3 Far, β-CH_2 Pal), 1.25−1.08 (m, 24H, 12 × CH_2 Pal), 0.89−0.75 (m, 9H, 2 × δ-CH_3 Leu, ω-CH_3 Pal); HPLC (RP-C4 from Macherey-Nagel; gradient [CH_3CN + 0.1% formic acid/H_2O + 0.1% formic acid]) 0 min, 50:50; 30 min, 100:0): t_R = 24.88 min; ESI-MS calcd for $[M + H]^+$ 1410.8, found 1410.5, calcd for $[M - H]^-$ 1408.8, found 1408.6.

Fluorescence Microscopy. A. Vesicle Preparation. *N*-Rh-DPPE (Lissamine rhodamine B, 1,2-dihexadecanoyl-*sn*-glycero-3-phosphoethanol-amine) (Figure 1B) was obtained from Molecular Probes (Eugene, OR). Stock solutions of phospholipids, cholesterol, and (**1**) were prepared in chloroform. The concentration of the lipid stock solutions was 0.2 mg/mL, and the molar ratio DMPC/DSPC was 1:1. For preparing giant unilamellar vesicles (GUVs), we followed the electroformation method developed by Angelova and Dimitrov.[35−37] To grow the GUVs, a special temperature-controlled chamber was used, which was previously described.[38] The experiments were carried out in the same chamber after vesicle formation, using an inverted microscope (Axiovert 35; Zeiss, Thornwood, NY). The following steps were used to prepare the GUVs. (1) The lipid solution (2 μL) was spread on each platinum (Pt) wire under a stream of N_2. To remove residues of the organic solvent, the samples were lyophilized for 1 h. (2) To add the aqueous solvent into the chamber (Millipore water, 17.5 MΩ cm), the bottom part of the chamber was sealed with a coverslip. The water was previously heated to 65 °C and then sufficient water was added to cover the Pt wires. After this step, the Pt wires were connected to a function generator (Hewlett-Packard, Santa Clara, CA), and a low-frequency AC field (sinusoidal wave function with a frequency of 10 Hz and an amplitude of 3 V) was applied for 90 min. After vesicle formation, the AC field was turned off and the temperature scan (from high to low temperatures) was initiated. A CCD color video camera (CCD-Iris; Sony, Tokyo) attached to the microscope was used to follow the vesicle formation and to select a target vesicle. The temperature was measured inside the sample chamber with a digital thermocouple (Model 400B; Omega, Stamford, CT) with a precision of 0.1 °C. The fluorescent probe and the peptide were premixed with the lipids in chloroform; the *N*-Rh-DPPE/lipid ratio used was 1:100 (mol/mol) and 1:400 (mol/mol) in the two-channel experiment.

B. Experimental Setup. The two-photon excitation microscopy experiments were performed at the Laboratory of Fluorescence Dynamics (University of Illinois at Urbana−Champaign). The high photon densities required for two-photon absorption are achieved by focusing a high peak power laser light source on a diffraction-limited spot through a high numerical aperture objective. Therefore, in the areas above and below the focal plane, two-photon absorption does not occur because of insufficient photon flux. This allows a sectioning effect without the use of emission pinholes as in confocal microscopy. Another advantage of two-photon excitation is the low extent of photobleaching and photodamage above and below the focal plane. For our experiments, we used a scanning two-photon fluorescence microscope[39,40] with an LDAchroplan 20× long working distance air objective (Zeiss, Homldale, NJ) with a numerical aperture of 0.4. A titanium-sapphire laser (Mira 900; Coherent, Palo Alto, CA), pumped by a frequency-doubled Nd:vanadate laser was used as excitation light source. The excitation

(35) Angelova, M. I.; Dimitrov, D. S. *Faraday Discuss. Chem. Soc.* **1986**, *81*, 303−311.
(36) Dimitrov, D. S.; Angelova, M. J. *Prog. Colloid Polym. Sci.* **1987**, *73*, 48−56.
(37) Angelova, M. I.; Soléau, S.; Meléard, Ph.; Faucon, J. F.; Bothorel, P. *Prog. Colloid Polym. Sci.* **1992**, *98*, 127−131.
(38) Bagatolli, L. A.; Gratton, E. *Biophys. J.* **1999**, *77*, 2090−2101.
(39) So, P. T. C.; French, T.; Yu W. M.; Berland, K. M.; Dong, C. Y.; Gratton, E. *Bioimaging* **1995**, *3*, 49−63.
(40) So, P. T. C.; French, T.; Yu, W. M.; Berland, K. M.; Dong, C. Y.; Gratton, E. *Two-photon fluorescence microscopy: Time-resolved and intensity imaging in fluorescence imaging spectroscopy and microscopy*; Wang, X. F., Herman, B., Eds.; Chemical Analysis series, Vol. 137; John Wiley and Sons: New York, 1996; pp 353−374.

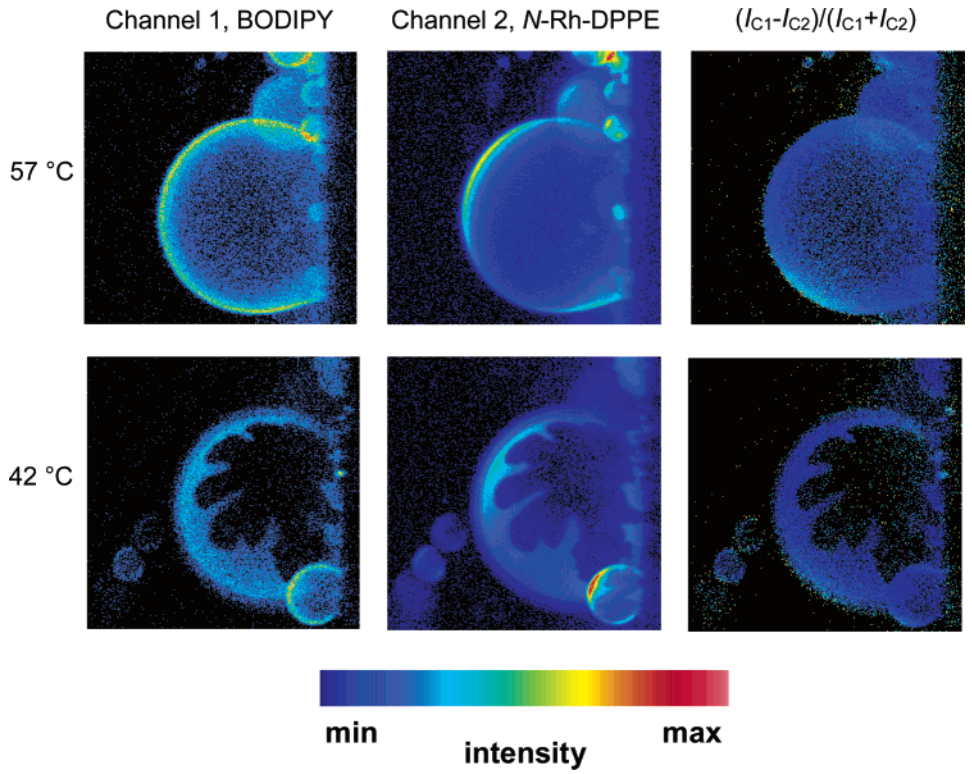

Figure 4. Two-photon excitation fluorescence intensity images (false color representation) of GUVs (size ~30 μm) consisting of DMPC/DSPC (1:1) + 2 mol % of peptide (**1**) + 0.25 mol % of *N*-Rh-DPPE. The intensity was collected in two channels, channel 1 detects the BODIPY fluorescence intensity and channel 2 the *N*-Rh-DPPE intensity, respectively. Images were taken at the top part of the GUVs at 57 and 42 °C.

wavelength was set at 780 nm. The laser was guided by a galvanometer-driven $x-y$ scanner (Cambridge Technology, Water-Town, MA) to achieve beam scanning in both the x and y directions. The scanning rate was controlled by the input signal from a frequency synthesizer (Hewlett-Packard, Santa Clara, CA), and a frame rate of 25 s was used to acquire the images (256 × 256 pixels). The fluorescence emission was observed through a broad band-pass filter from 350 to 600 nm (BG39 filter; Chroma Technology, Brattleboro, VT). For detecting both fluorophor emissions simultaneously in two channels, a fluorescein/Texas red filter set was used to collect fluorescence in the green and red regions, respectively. The green emission filter was a Chroma HQ525/50 (500−550 nm), the red was a Chroma HQ610/75 (573−648 nm), and the dichroic was a Q560LP. Both of the emission filters were coated for multiphoton work. A miniature photomultiplier (R5600-P; Hamamatsu, Brigdewater, NJ) was used for light detection in the photon counting mode. Figure 1C shows the normalized excitation and emission spectra of the *N*-Rh-DPPE and the peptide (**1**).

Fluorescence Spectroscopy. Emission spectra of the fluorophor BODIPY were obtained using the K2 multifrequency phase and modulation fluorometer with photon counting mode equipment (ISS Inc., Champaign, IL). The fluorometer uses a xenon arc lamp as a light source. The monochromator band-pass was 8 nm. The spectra were corrected for lamp intensity variation and monochromator efficiency. The excitation wavelength was 495 nm, and the emission spectra were collected from 510 to 700 nm in steps of 1 nm. The temperature was controlled to ±0.1 °C by a circulating water bath.

The fluorophor BODIPY (4,4-difluoro-4-borata-3a-azonia-4a-aza-*s*-indacene) is used for a wide range of different applications because of its exceptional spectral and photophysical stability compared to other fluorescent groups. In this study, we made use of the effect that BODIPY may form dimers, which can be identified by a strong (D_I band, at 477 nm) and weak (D_{II} band, at 570 nm) absorption band, which correspond to different conformations of the exciton coupled dimer state (sandwich-like vs collinear configuration). The monomer itself absorbs at about 500 nm. The integrated absorption band of D_I is about twice that of the monomer, which is compatible with exciton coupling within a dimer. Contrary to D_I, the D_{II} dimer is emitting light, as a broad band centered at about 630 nm.[41]

Results and Discussion

Fluorescence Microscopy. A. DMPC/DSPC. DSC, FT-IR, and SAXS data have shown that the gel−fluid coexistence region of the pure equimolar lipid mixture DMPC/DSPC appears between 30 and 49 °C.[11] Recently, we studied giant unilamellar vesicles (GUVs) of the pure lipid mixture using two different fluorophores (Laurdan and *N*-Rh-DPPE) in two-photon excitation fluorescence microscopy studies.[42] In the case of *N*-Rh-DPPE, the different probe partitioning between gel and fluid domains discriminates between fluid and gel-state domains. In the fluid phase of the lipid bilayer system, at $T \geq 49$ °C, the images obtained with *N*-Rh-DPPE as fluorophor show that the fluorescent molecules are distributed homogeneously on the vesicle surface (Figure 2). When the temperature is decreased to the gel−fluid two-phase coexistence region, nonfluorescent areas become visible on the vesicle surface showing lipid domain coexistence (Figure 2). The gel-type lipid domains expand and migrate around the vesicle surface as the temperature is further decreased. The gel-type domains span the inner and outer leaflets of the membrane, suggesting a strong coupling between the inner and outer monolayer of the lipid bilayer. Below 30 °C, as expected for an all-gel phase, the nonfluorescent regions disappear and an essentially homogeneous fluorescence distribution on the vesicle surface is observed.

(41) Bergstroem, F.; Mikhalyov, I.; Hagglof, P.; Wortmann, R.; Ny, T.; Johansson L. B.-A. *J. Am. Chem. Soc.* **2002**, *124*, 196−204.
(42) Fahsel, S.; Pospiech, E.-M.; Zein, M.; Hazlett, T. L.; Gratton, E.; Winter, R. *Biophys. J.* **2002**, *83*, 334−344.
(43) Bagatolli, L. A. *Chem. Phys. Lip.* **2003**, *122*, 137−145.

B. DMPC/DSPC/Peptide (1). Images in the fluid phase ($T \geq 49$ °C) of the lipid mixture with incorporated 2 mol % of the fluorescent lipidated peptide exhibit a homogeneous distribution of fluorescent molecules on the vesicle surface, similar to the system DMPC/DSPC with the fluorophor *N*-Rh-DPPE. With decreasing temperature, nonfluorescent areas become visible (Figure 3) and the shapes of these domains are very similar to the ones in the pure lipid mixture. To support our interpretation that these regions are the same gel-type lipid domains, we prepared vesicles with both fluorescent molecules, peptide (**1**) and *N*-Rh-DPPE, and detected the emission in two channels (Figure 4). At a temperature corresponding to the fluid phase of the lipid mixture, both emission channels show a homogeneous distribution of the fluorescence intensity. Decreasing the temperature to the gel−fluid two-phase region leads to the formation of domains with exactly the same size and shape in both channels. This is demonstrated by subtracting the intensities in both channels (Figure 4). As a result we can deduce that the lipidated peptide partitions essentially into the fluid phase of the lipid bilayer system. We also investigated the partitioning of the only palmitoylated and only farnesylated lipidated peptide into the binary lipid mixture. Both lipidated peptides partition essentially into the fluid phase of the lipid bilayer system, no significant partitioning into the gel domains is observed.

C. DMPC/DSPC/Cholesterol. To be able to tune additionally the lipid order parameter, acyl-chain length, and hence the packing density of the fluid phase, we added cholesterol up to levels of 33 mol %. At high temperature, in the overall fluid phase of the lipid mixture, the images of the lipid mixture with 20 mol % of cholesterol and *N*-Rh-DPPE as fluorophor display a homogeneous distribution of fluorescent molecules (Figure 5A). Interestingly, with decreasing temperature, no nonfluorescent domains are visible in the cholesterol-containing sample. No significant domain coexistence, at least in the μm range, remains in the temperature range where the gel−fluid coexistence region of the pure binary lipid mixture appears. Samples with cholesterol concentrations up to 10 mol % still exhibit small nonfluorescent areas (data not shown); large gel-type lipid domains are depleted at cholesterol concentrations higher than ~10 mol %, only.

D. DMPC/DSPC/Cholesterol/Peptide (1). Adding 2 mol % of the peptide to the phospholipid mixture with 20 mol % of cholesterol changes the pattern of lateral lipid organization. At high temperatures, in the fluid phase, the images still show a homogeneous distribution of the fluorescent peptide on the vesicle surface. With decreasing temperature, areas with higher fluorescence intensity become visible (Figure 5B), however. The domains are disk-shaped, which are indicative of fluid DMPC-rich domains with embedded peptide in a liquid-ordered, cholesterol-rich lipid environment. With further decrease of the temperature, these areas of a higher fluorescence intensity become continuously smaller and the fluorescence intensity increases concomitantly. At the lowest temperature employed, 30.8 °C, very small (~0.1 μm), very bright spots are visible on the vesicle surface. These images clearly indicate that incorporation of the peptide into a cholesterol-rich liquid-ordered phase is energetically unfavorable, and lipid sorting via peptide−lipid interactions is no longer a feasible process at these temperatures. As a consequence, condensation and aggregation of the fluorescent peptide molecules occurs at low temperatures, where a more gel-like ordered membrane environment is created. Evidence from spectroscopy experiments supports this conclusion (below).

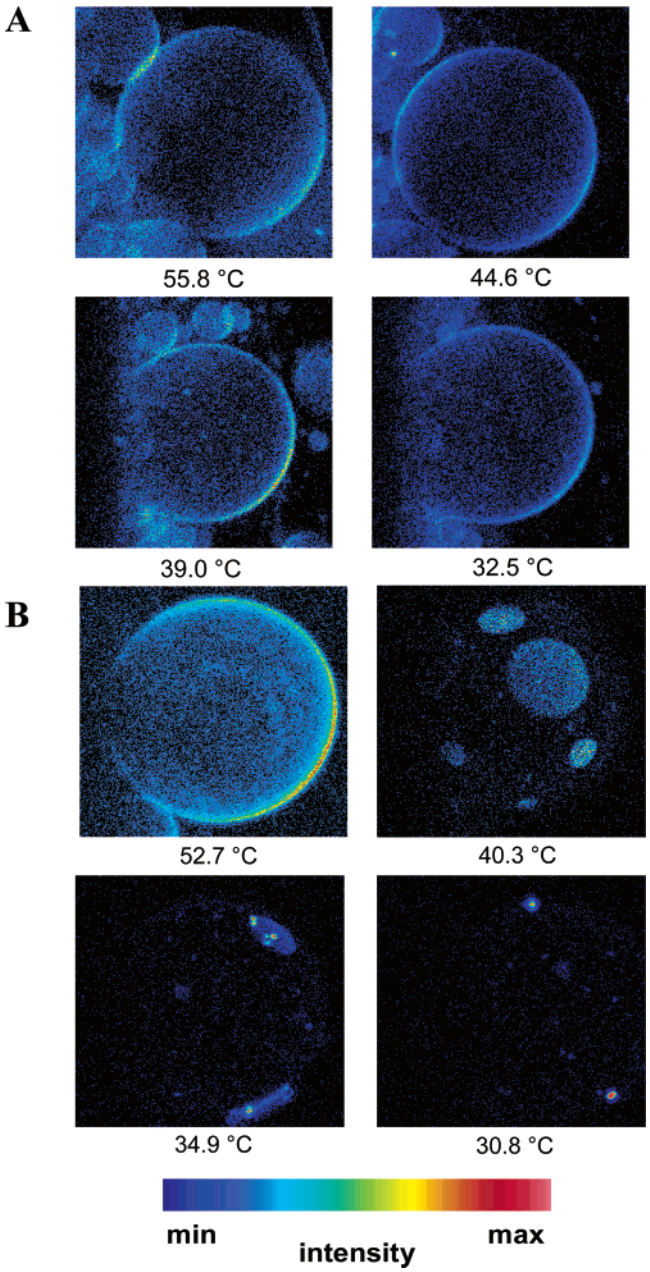

Figure 5. (A) Two-photon excitation fluorescence intensity images (false color representation) of GUVs (size ~30 μm) formed of DMPC/DSPC (1:1) + 20 mol % of cholesterol, labeled with *N*-Rh-DPPE. (B) Two-photon excitation fluorescence intensity images (false color representation) of GUVs (size ~30 μm) formed of DMPC/DSPC (1:1) + 20 mol % of cholesterol + 2 mol % of peptide (**1**). The images were taken at the top part of the GUVs at different temperatures.

Fluorescence Spectroscopy. Figure 6 shows the fluorescence emission spectra of the peptide incorporated in the mixture DMPC−DSPC (1:1) + 20 mol % of cholesterol at a concentration of 2 mol % as a function of temperature. At high temperature, only one emission maximum around 525 nm is visible, which is due to the monomer emission of the BODIPY fluorophor. With decreasing temperature, the intensity of the monomer emission decreases and a second emission maximum at about 625 nm emerges. At the lowest temperatures, the

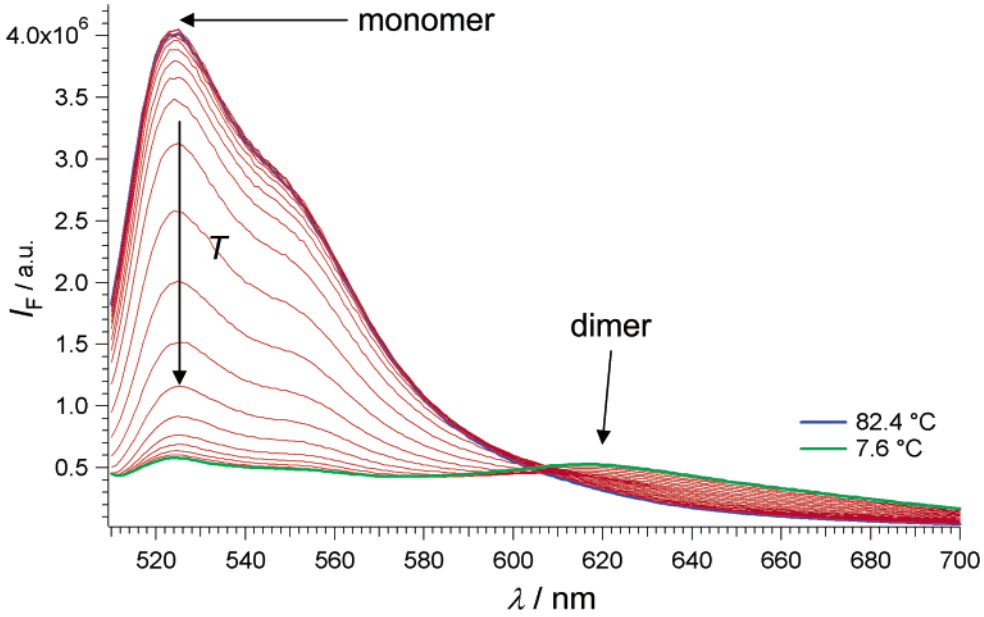

Figure 6. Emission spectra of DMPC/DSPC (1:1) + 20 mol % of cholesterol + 2 mol % of peptide (**1**) as a function of temperature (excitation wavelength 495 nm).

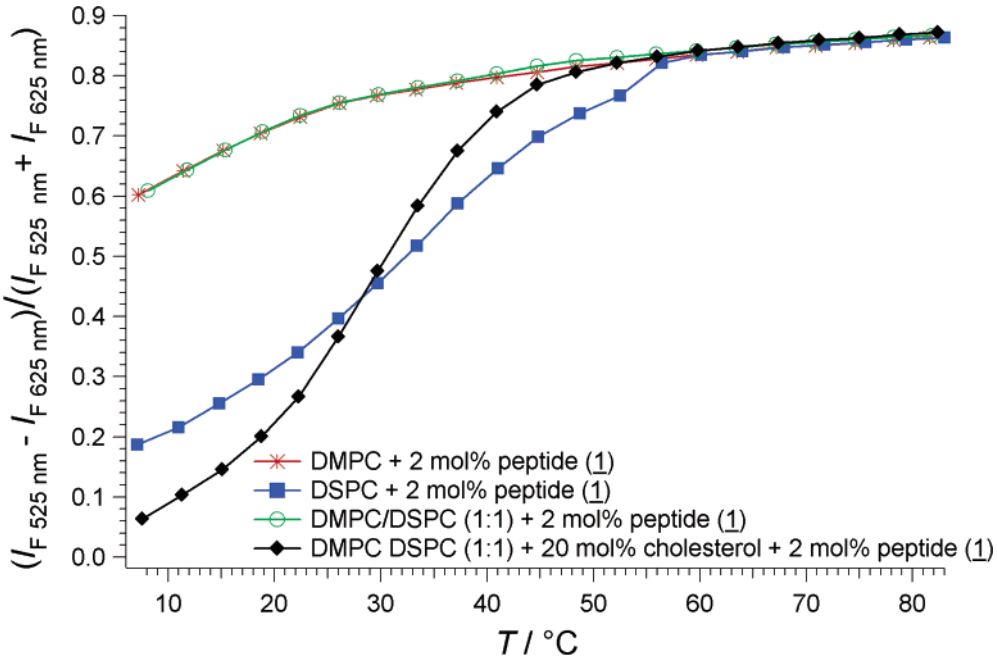

Figure 7. Monomer−dimer emission of the samples DMPC + 2 mol % of peptide (**1**), DSPC + 2 mol % peptide (**1**), DMPC/DSPC (1:1) + 2 mol % of peptide (**1**) and DMPC/DSPC (1:1) + 20 mol % of cholesterol + 2 mol % of peptide (**1**), respectively (main gel-to-fluid transition temperatures of the pure lipid components: DMPC 24 °C, DSPC 56 °C).

intensity of this red-shifted emission maximum is even higher than the emission intensity of the monomer. This can be explained by the fact that the BODIPY molecules form dimers which prevail at low temperatures and higher concentrations. The rapid drop of the fluorescence intensity at 525 nm with cooling is not followed by a concomitant strong increase of the intensity at 625 nm, as the transition dipole moments of both transitions are different. A more quantitative analysis is the possible application of a monomer/dimer two-state model using the intensities of the monomer and the dimer emission, normalized to the total intensity of both emission maxima. The relative intensity difference given in Figure 7 is proportional to the concentration of monomer species. The graph, which also displays the corresponding data for the pure lipid components, shows that the data for the samples DMPC + 2 mol % of peptide and DMPC/DSPC (1:1) + 2 mol % of peptide behave very similarly, revealing partitioning of the lipidated peptide essentially into the fluid DMPC-rich domains, only. The data of the sample DMPC/DSPC (1:1) + 20 mol % of cholesterol + 2 mol % of peptide at low temperatures are typical for the formation of a high population of BODIPY fluorescent dimers. Their concentration is even higher than that in the sample DSPC + 2 mol % of peptide at low temperature, which is known to be in an ordered, gel-like state below 56 °C. These data support the conclusion drawn from the microscopy data (above) that in the > 10 mol % cholesterol containing samples, regions with a

high concentration of the lipidated peptide are formed that become progressively smaller with decreasing temperature and lead to an increasing formation of BODIPY dimers.

Conclusions

We investigated the partitioning of the lipidated peptide (**1**) into the model biomembrane DMPC/DSPC (1:1) with and without incorporated cholesterol at different levels. In the system DMPC/DSPC (1:1) + 2 mol % of peptide, a homogeneous distribution of the peptide in the fluidlike membrane (at $T >$ 40 °C) is visible in the fluorescence microscopy images. Decreasing the temperature leads to the formation of nonfluorescent gel-type lipid domains with the same size and shape as in the pure lipid sample with the embedded fluorophor *N*-Rh-DPPE. The two-channel experiment shows that the peptide only partitions into the fluid, DMPC-rich domains of the membrane. The sample DMPC/DSPC (1:1) + 20 mol % of cholesterol exhibits a homogeneous distribution of fluorescence intensity not only in the fluidlike phase but also at lower temperatures down to about 30 °C: no large-scale gel-like domains are induced. Incorporation of cholesterol above levels of about 20 mol % leads to a depletion of large-scale concentration fluctuations and hence of the gel−fluid coexistence region. Adding 20 mol % of cholesterol to the system DMPC/DSPC (1:1) probably leads to the formation of a liquid-ordered phase over the entire temperature range. This is supported by the Laurdan general polarization values found for this system. Adding now 2 mol % of the peptide to this system greatly perturbs the lateral organization of the membrane. At a temperature corresponding to the fluid membrane, we still observe a homogeneous distribution of the peptide molecules on the vesicle surface. However, by decreasing the temperature, areas with higher fluorescence intensity become visible. These areas gradually become smaller with decreasing temperature until only small, bright spots remain at a temperature of ∼30 °C. The circular shape of the domains observed here (Figure 5B), which contrasts with the gel−fluid type domains seen in Figure 2, is typical for minimizing the area-to-perimeter ratio for isotropic phases in equilibrium. This kind of shape is also observed in model raft mixtures[42] that are thought to consist of liquid-ordered/liquid-disordered domains. These findings can be explained by a lipid sorting mechanism and phase separation on the vesicle surface induced by the polypeptide. By adding 2 mol % of the peptide to this membrane system, a phase separation is induced owing to the high affinity of the lipidated peptide to a fluid, DMPC-rich environment. This conclusion is supported by the shape of the domains and the decreasing population of these domains found with decreasing temperature. The phase separation leads to the formation of areas with higher fluorescence intensity, which become smaller and smaller with decreasing temperature. In these small domains, the local concentration of the peptide increases steadily and this leads to an increasing formation of BODIPY dimers, as observed in the fluorescence spectroscopy experiments. At the lowest temperatures, where the mean acyl-chain conformational order of the membrane has already drastically increased and hence gel-formation of the lipid bilayer membrane is strongly favored, an efficient lipid sorting mechanism is not feasible anymore. As a consequence, aggregation of the peptide in small clusters prevails. Hence, we can also conclude that in general the palmitoyl/farnesyl dual-lipidation motif found in proteins such as Ras may not promote significant association with liquid-ordered or gel-like domains in phase-separated bilayer membranes and therefore may also not partition into biological rafts. Our conclusions would also be consistent with results from fluorescence-quenching experiments on a family of *S*-palmitoyl/*S*-isoprenyl lipidated peptides carried out in other liquid-ordered/liquid-disordered phase-segregated model membrane systems.[26,33]

Acknowledgment. Financial support from the Deutsche Forschungsgemeinschaft and the Fonds der Chemischen Industrie is gratefully acknowledged. The fluorescence microscopy experiments reported in this paper were performed at the Laboratory for Fluorescence Dynamics (LFD) at the University of Illinois at Urbana−Champaign (UIUC). The LFD is supported jointly by the National Center for Research Resources of the National Institutes of Health (PHS 5 P41-RRO3155) and UIUC.

JA049922I